BNL 36833
CONF-8506125--8

BNL--36833

DE85 017510

INTERNAL FRICTION DUE TO DOMAIN-WALL MOTION IN MARTENSITICALLY TRANSFORMED A15 COMPOUNDS

C.L. Snead, Jr. and D.O. Welch
Brookhaven National Laboratory
Upton, NY 11973

DISCLAIMER

Resume -

Abstract - A lattice instability in A15 materials in some cases leads to a cubic-to-tetragonal martensitic transformation at low temperatures. The transformed material orients in lamellae with c axes alternately aligned along the <100> directions producing domain walls between the lamellae. An internal-friction (δ) feature below T_m is attributed to stress-induced domain-wall motion. The magnitude of the friction increases as temperature is lowered below T_m as $(1-c/a)$ increases, and behaves as $(1-c/a)^2$ from T_m down to the superconducting critical temperature where the increasing tetragonality is inhibited. The effect of strain in the lattice is to decrease the domain-wall internal friction, but not affect T_m. Neutron-induced disorder and the addition of some third-elements in alloying decrease both δ and T_m, with some elements reducing only the former. Less than 1 at. % H is seen to completely suppress both δ and T_m. Martensitically transformed V_2Zr demonstrates low-temperature internal-friction and modulus behavior consistent with easy β/m wall motion relative to the easy m/m motion of the A15's. For the V_2Zr, a peak in δ is observed, qualitatively in agreement with expected β/m wall motion.

INTRODUCTION

Although there has been a very large amount of work expended on studies of martensitic transformations, the understanding of the microscopic mechanisms involved so far is quite poor. To quote Planes et al. /1/ "In fact, only certain transitions - those found in the A15 compounds - can be explained in terms of microscopic properties of their constituents (it is believed that A15 compounds undergo a band Jahn-Teller transition /2-4/." Even with that, the microscopic mechanism giving rise to internal friction associated with the transformation is not known. This paper reviews some of the data on internal friction due to martensitic transformations in A15's, how various material treatments affect the friction, a "microscopic" theory to explain the friction, and how the data and the theory compare.

Some of the A15 compounds undergo a cubic-to-tetragonal martensitic transformation. This transformation is at temperature T_m below liquid-nitrogen temperature and above the superconducting critical temperature T_c. As with many martensitic transformations, it is associated with a lattice instability (the instability of the $\{110\}$ <110> mode with decreasing temperature and the vanishing of the shear modulus $(1/2)(C_{11}-C_{12})$ at T_m /5-6/. In Nb_3Sn the tetragonal-phase material is composed of twinned domains with c axes lying along <100> directions, and with the habit plane of the twin boundary along (110). At T_m, the c axis is reduced and the a and b axes equally lengthened. The tetragonality of the material increases, however, as the temperature is lowered below T_m as c/a decreases with decreasing temperature down to T_c where further change in c/a is arrested /2/. For Nb_3Sn at T_c, c/a = 0.9939 with T_m at 43 K /7/. On the other hand, V_3Si has the c axis larger than the a and b axes and a c/a of 1.0022 with a T_m of 21 K /7/. Note that the "tetroganality" $|(1-c/a)|$ of Nb_3Sn is roughly 3 times that of V_3Si at their respective T_c's.

The A15 superconductor Nb_3Sn is currently the prime material for the construction of magnets for applications such as confining magnets for fusion, and bending magnets for the Superconducting Supercollider. Since these applications require large stresses on the conductors, knowledge of the low-temperature modulus values and mechanical behavior is needed. The modulus data that are taken concomitantly with

the Q^{-1} data are, therefore, of scientific and engineering interest. As the transformation to the tetratragonal phase is thought to be intimately coupled with both mechanical behavior and to the superconducting critical properties, these studies take an added interest.

Figure 1 shows the internal friction of Nb_3Sn from 10-400 K. Specimens were polycrystalline 10-μm layers of Nb_3Sn sandwiching a 10-μm Nb substrate and cut into foils. Standard electrostatic drive in flexure was used at frequencies between 100 and 2000 Hz. The high-temperature peaks will be discussed later. The feature of note is the 2.5 order of magnitude increase in Q^{-1} between T_m (here 49 K) and T_c (18.1 K). (Data were taken for temperature ramps in both direction and no hysteresis or time dependence of Q^{-1} was ever detected. All data are shown for increasing temperature.) It is this feature that provides the means of studying various chemical and mechanical effects on the martensitic transformation.

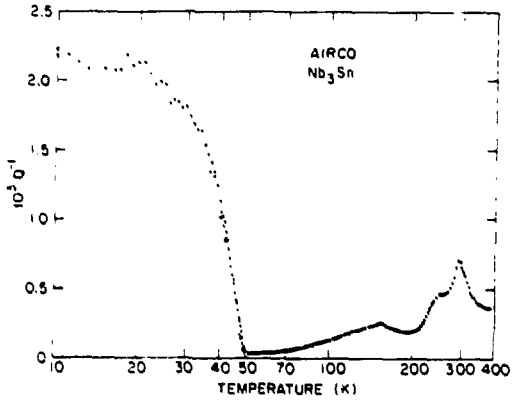

Fig. 1. Q^{-1} vs. temperature for "pure" Nb_3Sn foil.

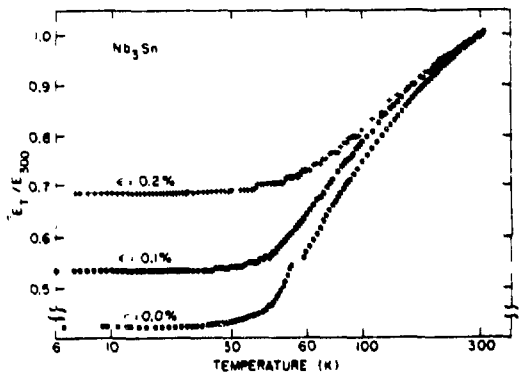

Fig. 2. Effect of internal strain in Nb_3Sn on the reduced modulus E(T)/E(300 K) as a function of temperature.

One of the first parameters investigated was the effect of strain on the transformation. Strain due to unrelieved deformation in the substrate was investigated as shown in the modulus measurements of Figure 2. Note that the modulus softens near T_m = 49 K to a value of ~40% of the room-temperature value in the strain-free specimen. This modulus softening reflects the instability of the $\{110\}\langle 110\rangle$ mode mentioned earlier. With increasing internal strain (ε=0.1 and 0.2%) the amount of softening is reduced significantly. Figure 3 shows the effects of this strain on the internal friction. The reduction in the friction with strain is considerable, but the main point to make is that even though the modulus and the internal friction are changed, the transformation temperature T_m is essentially unaltered, as is expected from a Landau-type theory of the transformation /8/.

The internal friction is attributed to the stress-induced motion of the martensitic/martensitic (m/m) domain walls with an attendant hysteretic loss. Microscopically, one envisions the reorientation of c axes from one <100> orientation to the twin <100> orientation as the twin boundary moves. In this way each atom (or unit cell) can be thought of as a "reorienting dipole". This interpretation is developed more fully in the Appendix. An important feature of that development is the prediction that the magnitude of the internal friction should vary as $(c/a-1)^2$. Two sets of "pure" Nb_3Sn data are fit with this expression with the data normalized at 18 K. There is one free parameter, T_m. Since c/a decreases with temperature, we use previously determined values /7/ in the fitting. The results are shown in Figure 4. The T_m value of 49 K, determined from the apparent highest-temperature of onset of the internal friction does not fit well. The value T_m = 44.5 K was found to give the best fit. Note that is near the value of 43 K usually associated with

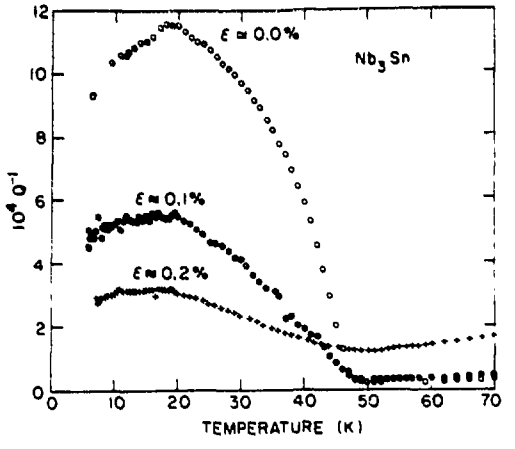

Fig. 3. Effect of strain on Q^{-1} as a function of temperature in Nb_3Sn.

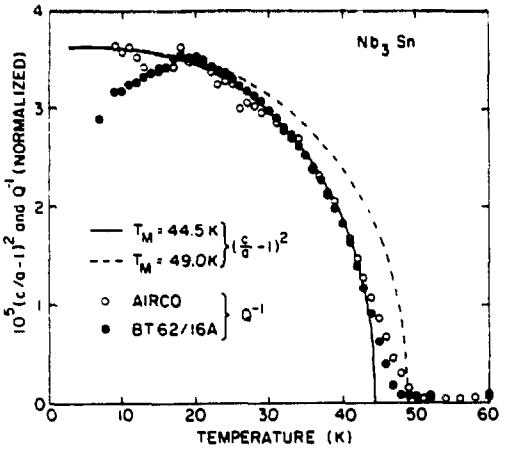

Fig. 4. Parametrized fit of $Q^{-1}\alpha\ (c/a-1)^2$ for the low-temperature internal friction of two Nb_3Sn specimens.

this transformation from X-ray work /7/. The region 44-49 K would then seem to be a temperature range denoting onset (49 K) and completion (44 K) of the cubic-to-tetragonal transformation. Below 44 K, all changes in Q^{-1} are attributed to changes in c/a. We will see that this transformation region below T_m can be broadened by different treatments.

A15 compounds with maximized critical properties are characterized as highly ordered compounds. The question has arisen of what the effects of disorder are on the compound's properties. Since these materials are envisioned to be used in radiation environments, for instance, the radiation-damage-induced disorder effects become of paramount importance. Figures 5 and 6 show the effects of 400 K reactor-spectrum neutron irradiation to Nb_3Sn. The primary defect produced affecting disorder from this irradiation is the antisite defect (A-B interchange in the A_3B compound) /9/. In Figure 5 there are three main things to note with regard to the disorder effects on the log decrement δ. The first is the decrease in δ with fluence. The second is the decrease in T_m with fluence. Recall that internal strain reduced δ but did not affect T_m at all. It is then clear that disorder plays a very different role in changing the characteristics of the transformation, most probably through the

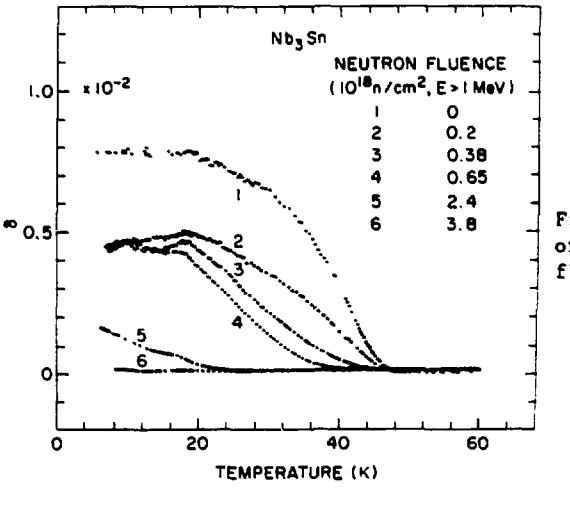

Fig. 5. Log decrement δ vs. temperature of Nb_3Sn for several reactor-spectrum fluences.

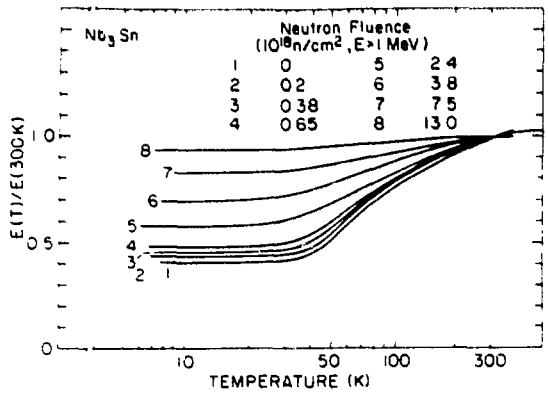

Fig. 6. Reduced modulus E(T)/E(300 K) vs. temperature of Nb_3Sn for several reactor-spectrum fluences.

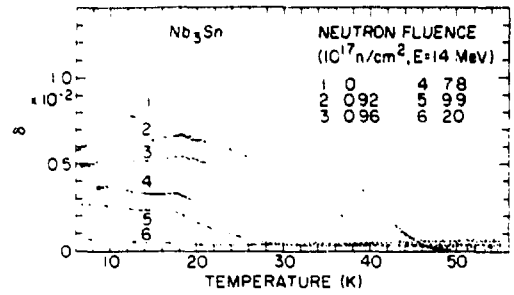

Fig. 7. Log decrement δ vs. temperature of Nb_3Sn for several fluences of 14-MeV neutrons.

electronic properties of the material which to first approximation are not affected by stress. T_m is seen to decrease monotonically (still present in the curve marked 6 if the scale is expanded and located at ~21 K). For fluences higher than 3.8×10^{18} n/cm^2, T_m would, by extrapolation, lie below T_c. Since c/a cannot change below T_c /2/, the transformation cannot, therefore; take place. Thus, disorder induced by neutron irradiation can completely arrest the martensitic transformation.

In addition to a reduction of δ and T_m with disorder, it is also noted from Figure 5 that as fluence (and disorder) increase, the shape of the δ curve between onset at high temperature and T_c changes from convex-right to convex-left: in other words, the $(1-c/a)^2$ dependence no longer holds. Indeed, the entire range for the 0.65×10^{18} n/cm^2 fluence takes on the character of the 44-49 K region of the unirradiated case. We think this is significant and that a fluctuation of disorder in the specimen creates the situation where a larger temperature range is spanned before the completion of transformation is realized. For curves 5 and 6 this temperature span clearly encompasses T_c.

The effect of increasing disorder on the mode softening and therefore the dynamic Young's modulus is shown in Figure 6. All the moduli are normalized to their respective values at 300 K. Softening of 60% for the "virgin" specimen is seen to decrease to only 6% for the 13×10^{18} n/cm^2 case. For the two highest fluences shown, there was no martensitic transformation. This significant increase in the low-temperature modulus in radiation environments could have important consequences in fusion applications. For the effect of pure 14-MeV neutrons on the transformation, Figure 7 shows the internal friction changes with fluence. Similar behavior to reactor-spectrum irradiation (Figure 5) is seen, but with an interesting difference. The changes of the superconducting T_c scale with damage energy when comparing the two types of neutron spectra (14-MeV neutron ~6 times more effective /10/), whereas the comparison here would give a value closer to 2.

Although Nb_3Sn is now the leading A15 candidate for high-field utilization, it is certain that for almost all applications the superconducting properties will be enhanced by the addition of one or more alloying addition, creating a "pseudobinary" compound. The question of how these additions might affect the martensitic transformation and therefore the basic critical properties, then arises.

The effects of adding Ti to the Nb_3Sn compound on the low-temperature internal friction are seen in Figure 8. Here it is noted that 3 at. % in the matrix completely suppresses the transformation by reducing T_m below T_c. As with neutron irradiation, Ti alloying reduces T_m and the magnitude of Q^{-1}. Both Q^{-1} and T_m

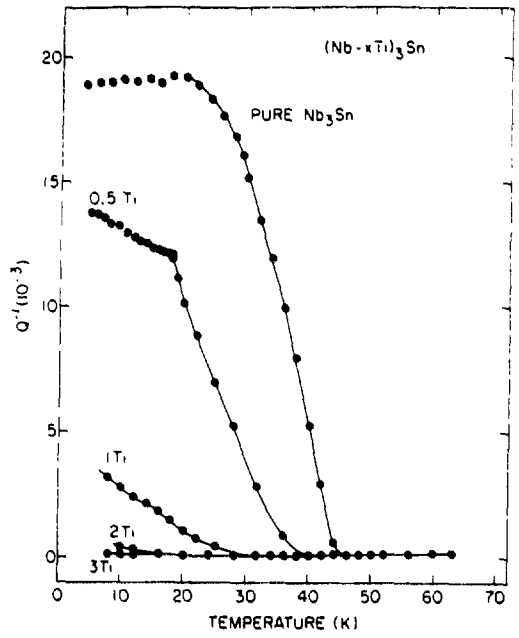

Fig. 8. Low-temperature Q^{-1} vs. temperature for Nb_3Sn + xTi for several values of x.

are similarly reduced by the alloying of a few percent of Ta but with T_m completely suppressed at the 7-at. % level, in comparison with 3 at. % for the Ti. It is to be noted that the introduction of Ti or Ta reduce both T_m and Q^{-1} due to domain-wall motion. The effects of Ti addition to the modulus is seen in Fig. 9 where the results are quite similar to those of the neutron-irradiated specimens.

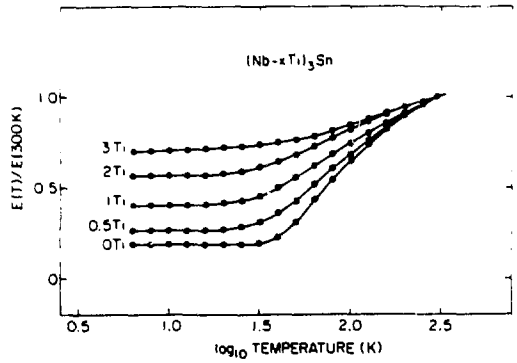

Fig. 9. Reduced modulus E(T)/E(300 K) vs. temperature for several concentrations of Ti in Nb_3Sn.

In continuing the study of third-element additions, an interesting departure from the behavior seen above was found. For the additions of Zr, the results shown in Fig. 10 were found. Here the low-temperature Q^{-1} is monotonically reduced by increasing levels of Zr, but T_m is unaffected. Further, the change in the curvature of Q^{-1} between T_m and T_c, seen earlier in the neutron-irradiated cases (and also in Fig. 8 for the Ti), is not evident here. This change in curvature was earlier attributed to a spread in the temperature range over which the transformation was taking place. For the Zr alloy, where T_m is not affected, this broadening of T_m does not obviously take place. Results similar to those of Zr are shown in Fig. 11 for Hf additions. The modulus curves for both of these alloys (Zr and Hf) are quite similar to those of Ti in Fig. 9, and are not shown.

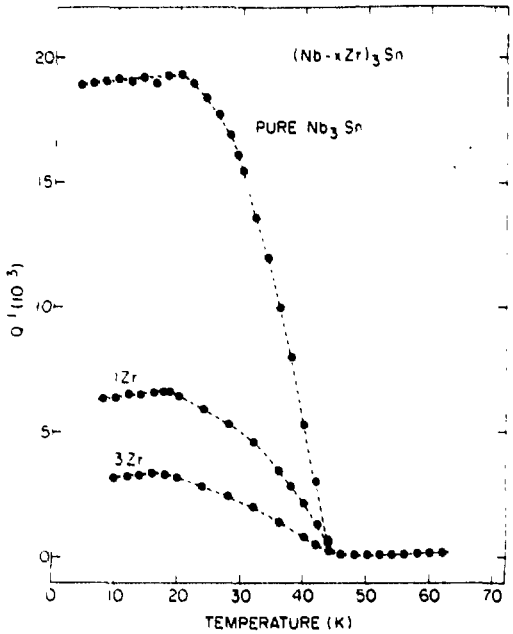

Fig. 10. Low-temperature Q^{-1} vs. temperature for Nb_3Sn + xZr for several values of x.

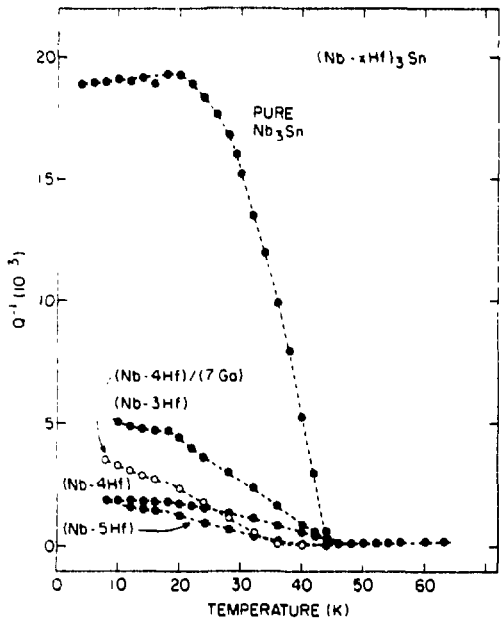

Fig. 11. Low-temperature Q^{-1} vs. temperature for Nb_3Sn + xHf for several values of x.

The difference in behavior of Q^{-1} and T_m for Ti and Ta additions on the one hand, and for Hf and Zr on the other are quite instructive. Where disorder is present in A15 compounds, whether by alloying, radiation damage, or deviation from stoichiometry, it is well known that the electrical properties (including the superconductivity critical properties) are much more sensitive to disorder on the A site than the B site./9/ The connection is then made to the alloying results here that it is probable that since Ti and Ta reduce T_m, but Hf and Zr do not, that Ti and Ta occupy the Nb sites, while Hf and Zr probably occupy the Sn sites since their presence does not suppress T_m. The EXAFS and TEM evidence for site occupation confirms the conjecture for the Ti and Ta: no definitive results for Hf or Zr are yet available. The major point regarding this is that we have here a possible new tool for identifying the site occupancy of dilute alloying additions, based upon internal-friction measurements.

Since the internal friction from the domain-wall motion is a clear indicator of the presence of transformed material, we also have a tool to test for the presence of the transformation in other A15 materials. Specimens of V_3Ga and Nb_3Ge have been tested. Fig. 12 shows the results for V_3Ga. First, the degree of modulus softening is about half of that of Nb_3Sn. The specimen is strain free and is near stoichiometry and perfect long-range order as attested by its value of T_c. Thus, we conclude from the lack of a low-temperature internal-friction feature (characteristic of twin-boundary motion) that V_3Ga probably does not undergo a martensitic phase transformation. Similar lack of internal friction in Nb_3Ge is rather inconclusive due to the substrate-induced strains and disorder in the specimens /11/.

There has been some work in the internal-friction effects of hydrogen in the A15's. Berry et al. /12/ investigated a relaxation peak associated with the presence of hydrogen. LeHuy et al. /13/ studied the effects of hydrogen charging on the martensitic transformation. The effects they found were very similar to those found by adding Ti or Ta: i.e., reduction of internal friction in the transformed regime and the reduction of T_m. The striking feature, however, is the complete suppression of T_m below T_c for hydrogen concentrations less than 1 at. % (see Fig. 13).

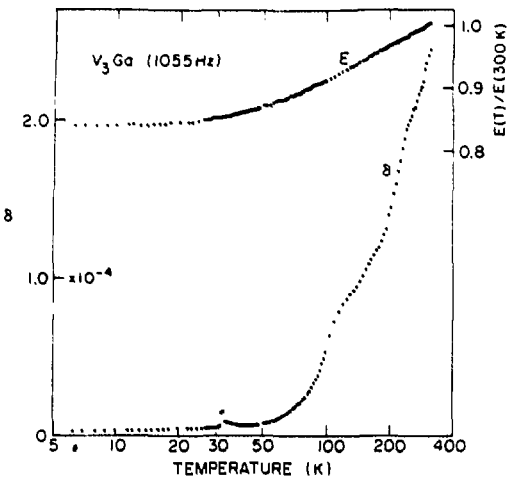

Fig. 12. Log decrement δ and reduced modulus E(T)/E(300 k) for V_3Ga.

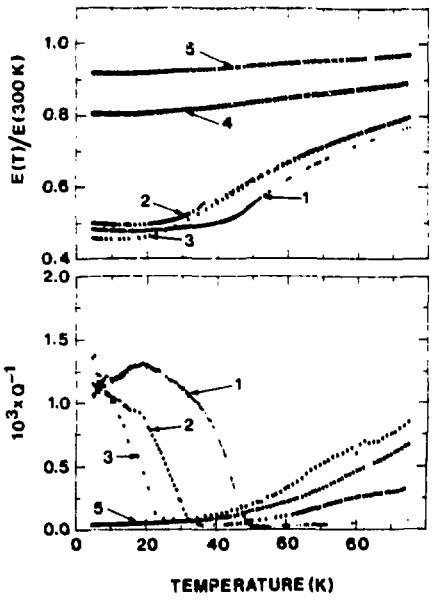

Fig. 13. Reduced modulus E(T)/E(300 K) vs. temperature (top) and Q^{-1} vs. temperature (bottom) for Nb_3Sn with various amounts of hydrogen: (1) None, (2) 0.2 at.%), (3) 0.15 at.%, (4) 1.8 at.%, and (5) 3.0 at. % (from LeHuy et al. /12/).

A departure from previous behavior is also noted that the reduction of softening (Fig. 13, top) does not scale with the reduction of T_m as with the metallic alloys. There are clearly different effects being manifested by the hydrogen inclusions that are not seen in other treatments. This would seem to be an interesting and fruitful area for further study.

For the A15 materials, we have only been concerned with internal friction due to the motion of twin boundaries that comprise the walls between differently oriented tetragonal domains. The presumption is that these boundaries move more easily under stress and/or have a much larger area than do any tetragonal/cubic (β/m) domain walls. Dejonghe et al. /14/ succinctly outlined the type of internal-friction response to be expected from the several possible types of domain-wall motion in thermoelastically transforming specimens. The A15 results fit the case of easy m/m boundary motion, with little or no β/m contribution. The other major possibility for friction involves the case where β/m motion is predominant: cases where the threshold stress for m/m motion is higher than that for β/m, or due to the lack of m/m interfaces.

For the case of β/m interface motion, instead of constant (or increasing with c/a) friction below T_m, a (ill defined) peak is expected below T_m. Also other effects such as heating-rate dependencies, hysteresis, etc. are to be expected. An example of this kind of phenomenon is shown in Fig. 14 for V_2Zr (Laves phase or C15 structure) which undergoes a cubic-to-rhombohedral transformation at a 116 K. The data here were taken for an increasing temperature ramp of ~1 K/min. Two features are to be noted that contrast with the A15 results. The "peak" in the interval friction argues for β/m domain-wall motion, with no evidence for any m/m contribution. Also, the modulus begins to show hardening due to the transformed material, which is fully in keeping with expected behavior. Recall, that the A15's show no such hardening below T_m, and this lack of hardening is ascribed to a modulus effect due to the easy motion of the m/m domains. The hardening in the

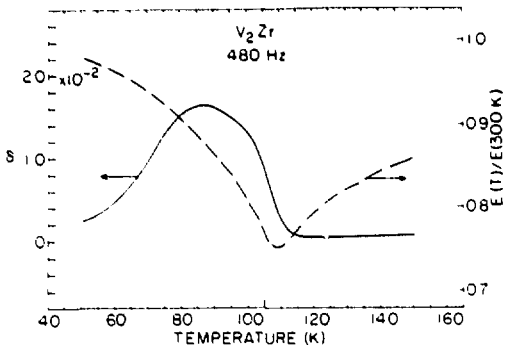

Fig. 14. Log decrement δ vs. temperature for V_2Zr in region 2 the martensitic transformation. Reduced modulus E(T)/E(300 K) is also plotted.

V_2Zr, then, is further evidence of the lack of a m/m loss mechanism being present in this system. This V_2Zr system also displays a marked hysteretic and heating dependence of the internal friction, that is consistent with ß/m wall motion (L. Snead, to be published).

CONCLUSIONS

The martensitic phase transition Nb_3Sn and its alloys has been shown to give rise to a large internal friction (Q^{-1}). Presumably other A15 compounds, such as V_3Si, which have this type of transition will also manifest this internal friction. (However, the magnitude of Q^{-1} seems to vary with $(c/a - 1)^2$; thus the magnitude for V_3Si should be a factor of about 8 smaller than that for Nb_3Sn.) The characteristics of the internal friction, such as the dependence on $(c/a - 1)^2$, are consistent with it being caused by the stress-induced motion of the boundaries (domain walls) between different variants of the tetragonal phase. Furthermore, these domain walls seem to be able to move relatively freely under the influence of the stress, but further understanding of the dynamics of domain-wall motion require additional experiments to characterize the stress-amplitude and frequency dependence

of the internal friction. Both the internal friction strength and the softening of the elastic modulus associated with the martensitic phase transition were shown to depend sensitively on the state of stress, the degree of disorder, the presence of solutes, and other factors; thus they will provide useful tools for the further investigation of this interesting phase transition in an important class of intermetallic compounds.

ACKNOWLEDGMENTS

This research was performed under the auspices of the U.S. Department of Energy, Division of Materials Sciences, Office of Basic Energy Sciences under Contract No. DE-AC02-76CH00016.

The experimental work presented here is largely the product of several collaborations and independent studies. The major people included were J. Bussiere, B. Berry, B. Faucher, H. Kumakura, and M. Suenaga. The technical assistance of B. Jones and W. Tremel is greatly appreciated.

APPENDIX A. Simple Model for the Low-Temperature Internal Friction and Modulus Defect in A15 Compounds

Consider a sample consisting of material tranformed into the tetragonal phase, with volume fraction f_t, as well as, possibly, some untransformed material in the cubic phase, with volume fraction $(1-f_t)$. The transformed material consists of domains of the three possible variants of the tetragonal phase (i.e., with the c axis along either the x, y, or z axes); the volume fraction of each of the different types of domain will be denoted by f_x, f_y, and f_z, with $f_t = f_x + f_y + f_z$. We assume, for simplicity, that the applied stress used in the measurement of the

dynamic modulus does not alter the total amount of transformed material, so that f_t is a constant. Furthermore, we assume that the elastic strain induced in an individual domain is much smaller than the tetragonality (c/a-1) caused by the martensitic transformation.

Again for simplicity, consider the effect of an oscillating uniaxial tensile stress along the z axis:

$$\sigma_{zz} = \sigma_o e^{i\omega t} . \tag{1}$$

This will induce a component of strain along the z axis, which also oscillates (but not necessarily in phase with σ_{zz}):

$$\varepsilon_{zz} = \langle E_o^{-1} \rangle \sigma_{zz} + \Delta f_z \left(\frac{c}{a} - 1\right) , \tag{2}$$

where the first term represents the instantaneous elastic strain and the second is the contribution due to domain-wall motion. E_o is the unrelaxed Young's modulus, while the angular brackets represent a volume average over the various domains as well as the untransformed material. Δf_z is the time-dependent change in the volume fraction of z axis domains produced by the consumption or creation of adjacent x- and y-axis domains by domain-wall motion. The internal friction, Q^{-1}, and Young's modulus E, are obtained by standard methods /15/ from the in-phase and out-of-phase components of $\varepsilon_{zz}/\sigma_{zz}$:

$$Q^{-1} = \frac{-2\pi \left(\frac{c}{a} - 1\right) \mathrm{Im}\,(\Delta f_z/\sigma_{zz})}{E^{-1}} , \text{ and} \tag{3}$$

$$E^{-1} = \langle E_o^{-1} \rangle + \left(\frac{c}{a} - 1\right) \mathrm{Re}\,(\Delta f_z/\sigma_{zz}) . \tag{4}$$

The required change in z-domain volume fraction, Δf_z, is a complex quantity with the relative contribution of its real and imaginary parts dependent on the details of domain-wall dynamics, about which more later. If however, in general the dynamic response of the domain populations to an applied stress will be of the form:

$$\Delta f_z \propto F(\sigma_{zz}) \cdot R(\omega) \cdot A ,$$

where $F(\sigma_{zz})$ is the (thermodynamic) force on a domain wall caused by the stress σ_{zz}, $R(\omega)$ is a frequency-dependent response function which depends on the mechanism of domain-wall motion, and A is the domain-wall area per unit volume. The force F is found from the change in the elastic thermodynamic potential of the crystal caused by the displacement of the wall separating two types of domain (e.g., x domain and a z domain); this may be found using the explicit expressions for the elastic thermodynamic potentials of the three types of domain given by Pietrass./16/ Thus:

$$F(\sigma_{zz}) = g\, \sigma_{zz} \left(\frac{c}{a} - 1\right) v_d^{2/3} ,$$

where g is a numerical factor which depends on the geometrical shape of the domains, and v_d is the average domain volume. Consequently, the internal friction and Young's modulus are given by:

$$Q^{-1} = - \frac{2\pi\, \alpha \left(\frac{c}{a} - 1\right)^2 f_t\, v_d^{1/3}}{E^{-1}} \mathrm{Im}\, R(\omega) \tag{5}$$

and

$$E^{-1} = \langle E_0^{-1} \rangle + \alpha \left(\frac{c}{a} - 1\right)^2 f_t \, v_d^{1/3} \, \mathrm{Re}\, R(\omega) \,, \tag{6}$$

where α is a numerical factor which depends on the domain shape. It is seen from Eq. (5) that the internal friction is proportional to $(c/a-1)^2$, and this is observed experimentally as shown in Figure 4. Basically, the factor $(c/a-1)^2$ arises because the strain produced when a domain wall moves is proportional to $(c/a-1)$. The product of these two factors enters into Q^{-1}, which is therefore proportional to $(c/a-1)^2$. Note that the fact that the temperature dependence of Q^{-1} is essentially accounted for by that of $(c/a-1)^2$ implies that the frequency response function $R(\omega)$, and hence the domain-wall mobility, must depend only weakly on temperature.

A specification of the frequency dependence of the internal friction, Q^{-1}, and the modulus defect, $\langle E_0^{-1}\rangle^{-1}$-E, requires an explicit model for the domain-wall dynamics so that the response function $R(\omega)$ can be evaluated. For example, if domain walls are reasonably mobile over most of their extent, except for certain edges, corners, etc., where they are highly pinned (by, for example, interactions with grain boundaries, intersecting with other domain walls, etc.), and if there is no critical stress which must be overcome prior to motion, as discussed by DeJonghe et al. /14/, then a damped-harmonic-oscillator model of domain-wall dynamics may be appropriate. (A recent theoretical study of domain-wall motions in A15 compounds by Barsch and Krumhansl /17/ suggests that these walls behave as solitons, and thus they should not have strong "Peierls-Nabarro"-type critical stresses required to set them moving.) In such a harmonic model, domain walls will be characterized by an effective mass m, resonance frequency ω_0, and viscous-damping coefficient κ (to account for damping by electron scattering, phonon emissions, etc.), the dynamics will then be characterized by:

$$m\ddot{x} + \kappa \dot{x} + m\omega_0^2 x = F(t) \tag{7}$$

where x is the boundary displacement caused by a force F. Such dynamics lead to the response function:

$$R(\omega) = \left(\frac{m(\omega_0^2 - \omega^2) - i\,\kappa\omega}{m^2(\omega_0^2 - \omega^2)^2 + \kappa^2\omega^2}\right). \tag{8}$$

The frequency depedence levels of the internal friction and modulus defect for the damped-harmonic-oscillator model of domain-wall dynamics are then obtained by combining Eq. (8) with Eqs. (5) and (6). Further experiments are required to test the predictions of this model.

REFERENCES

1. A. Planes, J. Vinals, and V. Torra, Phil. Mag A. 48, 501 (1983).

2. R. N Bhatt and W. L. McMillan, Phys. Rev. B 14, 1007 (1976).

3. R. N. Bhatt, Phys. Rev. B 17, 2947 (1978).

4. B. Luthi and W. Rehwald, Structural Phase Transitions, ed. by K. A. Müller and H. Thomas, Springer-Verlag, 1978, p. 131.

5. L. R. Testardi in Physical Acoustics, ed. by W. P. Mason and R. N. Thurston (Academic Press, NY), Vol X, p. 193; Vol XIII, p. 29 (1973).

6. M. Weger and I.B. Goldberg, in Solid State Physics, ed. by F. Seitz and D. Turnbull (Academic Press, NY), Vol. 28, p. 1 (1973).

7. R. Mailfert, b.W. Batterman, and J.S. Hanak, Phys. Stat. Sol. 32, K67 (1969).

8. D. O. Welch, Advances in Cryogenic Engineering - Materials, ed. by R.P. Reed and A.F. Clark, (Plenum press, NY), Vol. 28, 1982, p. 655.

9. A. R. Sweedler, C.L. Snead, Jr., and D. E. Cox, Treatise on Materials Science and Technology, ed. by T. Luhman and D. Dew-Hughes (Academic Press, NY), Vol. 14, 1979, p. 349.

10. C. L. Snead, Jr., D. M. Parkin, and M. W. Guinan, J. Nucl. Mat. 103 and 104, 749 (1981).

11. C. L. Snead, Jr. and J. F. Bussiere, Phil. Mag. (accepted for publication).

12. B. S. Berry, W. C. Pritchet, and J.F. Bussiere, Scripta Met. 17, 327 (1983).

13. H. LeHuy, J. F. Bussiere, and B. S. Berry, IEEE Trans. Magn. MAG-19, 893 (1983).

14. W. Dejonge, R. deBatist, and L. Delaey, Scripta Met 10, 1125 (1976).

15. A. S. Nowick and B. S. Berry, Anelastic Relaxation in Crystalline Solids, (Academic Press, NY), 1972.

16. B. Pietrass, Phys. Stat. Sol. (V) 68, 553 (1975).

17. G. K. Barsch and J. A. Krumhansl, Phys. Rev. Lett. 53, 1069 (1984).